DEVELOPMENT AND TESTING OF A NEW MECHANISTIC MODEL FOR MULTIPHASE FLOW IN PIPES

Nicholas Petalas
Petroleum Engineering Department
Stanford University
Stanford, California

Khalid Aziz
Petroleum Engineering Department
Stanford University
Stanford, California

This paper was prepared for presentation at the ASME Fluids Engineering Division Second International Symposium on Numerical Methods for Multiphase Flows held at San Diego on July 7-11, 1996.

ABSTRACT

The use of mechanistic models for multiphase flow calculations is expected to greatly improve our ability to predict pressure drop and holdup in pipes. In this paper, a new model is developed which can be used for all pipe geometries and fluid properties. The model lends itself to implementation in a computer program in that a significant number of calculations are required and several of these require iterative procedures. The performance of the model over a wide range of conditions has been evaluated through the use of three dimensional surface plots. Comparisons with laboratory as well as field data have also exhibited good results. This work has also identified the need for further work in this area.

INTRODUCTION

Empirical models often prove inadequate in that they are limited by the range of data on which they were based and, generally, cannot be used with confidence with the types of fluids or under the types of conditions encountered in the field. Furthermore, many such models exhibit large discontinuities[4] at the flow pattern transitions and this can lead to convergence problems when these models are used for the simultaneous simulation of petroleum reservoirs and associated production facilities. Mechanistic models, on the other hand, are based on fundamental laws and thus can provide for more accurate modeling of the geometric and fluid property variations. Most mechanistic models begin by assuming that a particular flow regime is present. By solving the momentum balance equations for certain quantities that determine its characteristics, the stability of the flow pattern is examined. If the chosen flow pattern is shown to be stable, the procedure is terminated, the pressure drop and phase volume fractions being obtained directly from the momentum balance equations. If the flow pattern cannot exist under the specified conditions, a new flow pattern is assumed and the procedure is repeated until a stable flow pattern is determined.

To date, many of the models presented in the literature are either incomplete[6),15)], in that they only consider flow pattern determination, or are limited in their applicability to all pipe inclinations[3),18)]. A new model has been developed which overcomes these limitations.

For most of the flow patterns considered, one or more empirical closure relationships are required even when a mechanistic approach is used. Where correlations available in the literature are inadequate for use in such models, new correlations must be developed.

A large amount of data has been collected through the use of a Multiphase Flow Database developed at Stanford University. This database program allows the user to specify criteria which limit the range of data selected and to output the results using a number of different formats. The database presently contains over 20,000 laboratory measurements and approximately 1800 measurements from actual wells. The required empirical correlations were developed based on these data and they reflect changes in pipe diameter, fluid properties and pipe inclination (upward and downward inclinations are represented).

MODEL DESCRIPTION

The development of mechanistic models to predict the behavior of multiphase systems started with the pioneering work of Taitel and Dukler[15] (1976). While they dealt only with flow pattern predictions, these ideas have been extended here to obtain comprehensive design techniques. The basic flow patterns considered in this approach are:

- Stratified Smooth
- Stratified Wavy
- Intermittent (slug, elongated bubble, plug)
- Annular Mist (annular flow with dispersed bubbles)
- Bubble
- Dispersed Bubble
- Froth or Churn

Equilibrium Stratified Flow

The geometrical aspects of this kind of flow are shown in Figure 1.

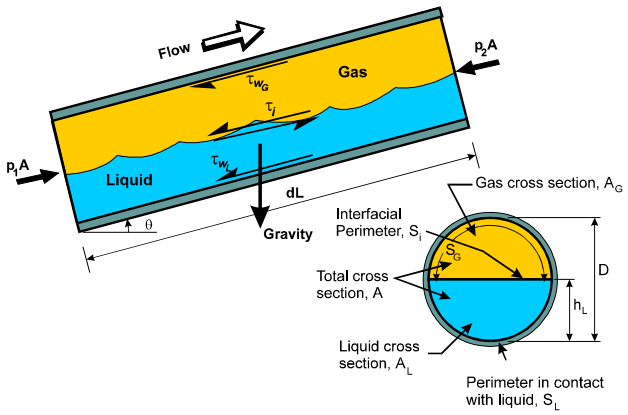

FIGURE 1 - MOMENTUM BALANCE WITH TWO SEGREGATED FLUIDS

Momentum balance can be written on the liquid and gas phases contained in a control volume. After taking the limit as ΔL→0 the two momentum balance equations may be expressed as:

$$-A_L\left(\frac{dp}{dL}\right)-\tau_{wL}S_L+\tau_i S_i-\rho_L A_L\frac{g}{g_c}\sin\theta=0 \qquad \text{Eq. 1}$$

and

$$-A_G\left(\frac{dp}{dL}\right)-\tau_{wG}S_G-\tau_i S_i-\rho_G A_G\frac{g}{g_c}\sin\theta=0 \qquad \text{Eq. 2}$$

The shear stress terms can be expressed in terms of friction factors:

$$\tau_{wL}=\frac{f_L\rho_L V_L^2}{2g_c},\ \tau_{wG}=\frac{f_G\rho_G V_G^2}{2g_c},\ \text{and}\ \tau_i=\frac{f_i\rho_G V_i|V_i|}{2g_c} \qquad \text{Eq. 3}$$

The friction factors for the gas and liquid phases are evaluated from the single phase relationships by using the Colebrook[9] correlation with the following definitions of Reynolds number and hydraulic diameter:

$$\mathrm{Re}_L=\frac{D_L\rho_L V_L}{\mu_L},\ D_L=\frac{4A_L}{S_L} \qquad \text{Eq. 4}$$

$$\mathrm{Re}_G=\frac{D_G\rho_G V_G}{\mu_G},\ D_G=\frac{4A_G}{S_G+S_i} \qquad \text{Eq. 5}$$

Following the approach used by Taitel and Dukler,[15] the momentum balance equations can be combined and expressed in dimensionless form leading to the following expression which can be solved to determine the equilibrium liquid height:

$$X^2F_2-F_1+4Y=0 \qquad \text{Eq. 6}$$

The quantity, X, is the Lockhart-Martinelli parameter:

$$X^2=\frac{\left(\frac{dp}{dL}\right)_{SL}}{\left(\frac{dp}{dL}\right)_{SG}}=\frac{f_{SL}V_{SL}^2\rho_L}{f_{SG}V_{SG}^2\rho_G} \qquad \text{Eq. 7}$$

The remaining quantities are given by:

$$Y=\frac{(\rho_L-\rho_G)g\sin\theta}{\left(\frac{dp}{dL}\right)_{SG}g_c} \qquad \text{Eq. 8}$$

$$F_1=\left(\frac{f_G}{f_{SG}}\right)\tilde{V}_G^2\left\{\frac{\tilde{S}_G}{\tilde{A}_G}+\frac{f_i}{f_G}\frac{\tilde{V}_i^2}{\tilde{V}_G^2}\left(\frac{\tilde{S}_i}{\tilde{A}_G}+\frac{\tilde{S}_i}{\tilde{A}_L}\right)\right\} \qquad \text{Eq. 9}$$

$$F_2=\left(\frac{f_L}{f_{SL}}\right)\tilde{V}_L^2\frac{\tilde{S}_L}{\tilde{A}_L} \qquad \text{Eq. 10}$$

Normally it is assumed that the superficial gas velocity is much higher than the interface velocity. This simplification however, is only valid for horizontal or uphill flow where gas moves much faster than liquid. To provide for a more general application, here it is assumed that the interface velocity is given by the difference of the average phase velocities, i.e.

$$V_i=(V_G-V_L) \qquad \text{Eq. 11}$$

The interfacial friction factor is obtained from the modification of the Duns and Ros method by Baker et al[5].

The simplifications imposed by Taitel and Dukler, i.e., that $f_i\approx f_G$, $V_G>>V_L$, and that the friction factors can be approximated by the smooth-pipe correlation of Blasius, limit the applicability of their model and are not made in this model. Furthermore, since the values of X and Y are dependent on pressure gradients, which are in turn dependent on pipe roughness, the evaluation of the effect of roughness based on dimensionless plots of liquid height versus X for various values of Y is not trivial. An iterative procedure is required where for a given value of Y, the value of X required to obtain a desired dimensionless liquid height is determined. The results thus obtained are relevant only for the specific set of fluid properties and pipe roughness analyzed. Our results show that the effect of roughness can be significant, even for very small values of Y.

The stability of the stratified flow pattern can be determined once the liquid height is known. The approach used by Taitel and Dukler, using an extension of the Kevin-Helmholtz wave stability theory is also used in this model. This attempts to predict the gas velocity at which waves on the liquid surface are large enough to bridge the pipe:

$$V_G=\left(1-\frac{h_L}{D}\right)\sqrt{\frac{(\rho_L-\rho_G)gA_G\cos\theta}{\rho_G\frac{dA_L}{dh_L}}} \qquad \text{Eq. 12}$$

or, in dimensionless form:

$$F^2\left[\frac{\tilde{V}_G^2}{(1-\tilde{h}_L)^2\tilde{A}_G}\frac{d\tilde{A}_L}{d\tilde{h}_L}\right]\geq 1 \text{ where} \qquad \text{Eq. 13}$$

$$F=\frac{V_{SG}}{\sqrt{Dg\cos\theta}}\sqrt{\frac{\rho_G}{\rho_L-\rho_G}},\ \frac{d\tilde{A}_L}{d\tilde{h}_L}=\sqrt{1-\left(2\tilde{h}_L-1\right)^2}$$

Xiao[18] et al. suggest that this mechanism of wave growth for the transition to intermittent flow may not be applicable for large diameter pipes where the entrainment deposition process is more dominant. At steep downward inclinations, Barnea[6] proposes a mechanism whereby stratified flow can change to annular, even at relatively low gas rates. This occurs when the liquid height is small and the liquid velocity is high. Liquid droplets are sheared off from the wavy interface and may be deposited on the upper pipe wall, eventually developing into an annular film. The condition for this type of annular flow is given as:

$$V_L>\sqrt{\frac{gD(1-\tilde{h}_L)\cos\theta}{f_L}} \qquad \text{Eq. 14}$$

Although no distinction is made in this model between stratified smooth and stratified wavy flow for the purposes of determining

pressure drop and liquid volume fraction, the transition between these two regimes is considered. Taitel and Dukler propose that waves will form on the liquid surface once the gas velocity is increased beyond:

$$V_G \geq \sqrt{\frac{4\mu_L(\rho_L-\rho_G)g\cos\theta}{s\rho_L\rho_G V_L}} \qquad \text{Eq. 15}$$

where the sheltering coefficient, s, is given as 0.01. Xiao et al. and in the present model, s is taken as 0.06, based on a study by Andritsos[1]. This value is said to be more suitable, especially for gas flow with high viscosity liquids.

During downflow, waves can develop on the flowing liquid even in the absence of interfacial shear from the gas flow. The criterion for the appearance of waves can be expressed in terms of a critical Froude number which varies from 0.5 to 2.2 depending on roughness and whether the flow is laminar or turbulent. Barnea[6] recommends a limiting value of 1.5 for the critical Froude number. When interfacial effects are considered in the calculation of the liquid height, this limit can predict smooth flow even at high liquid rates where the flow is known to be wavy. Reducing the limit to 1.4 resolves this problem. Thus the transition from stratified smooth to wavy flow based on this mechanism is:

$$\mathrm{Fr} = \frac{V_L}{\sqrt{gh_L}} > 1.4 \qquad \text{Eq. 16}$$

Barnea also notes that theory and experiment both suggest that stratified smooth flow does not exist for downward inclinations greater than ~5°.

The solution of the momentum balance equations produces multiple roots when the pipe inclination is positive. Xiao et al.[5] assume that the lowest root is the physical one. It has been observed however, that in certain circumstances the roots are in close proximity and it is not possible to discern which root is the physical one. It is believed that the cause of the multiple root phenomenon and our inability to establish which of the roots is the physical one is perhaps due to the inadequacies of the stratified flow model. For this reason, the present model limits stratified flow to horizontal and downhill angles only.

If the flow is shown to be stratified, the liquid volume fraction may be evaluated from:

$$E_L = \frac{A_L}{A} = \frac{4\tilde{A}_L}{\pi} \qquad \text{Eq. 17}$$

The pressure drop can be obtained directly from either one of the momentum balance equations (Eq. 1 or Eq. 2).

Annular Mist Flow

The approach presented here is based on the work of Oliemans[13] et al. (1986), and Xiao[18] et al. (1990), who in turn have used the work of many previous investigators. The model is based on the assumption of a constant film thickness and no slip between the liquid droplets in the gas core and the gas phase. It does however account for the entrainment of the liquid in the gas core (Figure 2).

Momentum balance on the liquid film and gas core with liquid droplets yields:

$$-A_f\left(\frac{dp}{dL}\right) - \tau_{wL}S_L + \tau_i S_i - \rho_L A_f \frac{g}{g_c}\sin\theta = 0 \qquad \text{Eq. 18}$$

and

$$-A_c\left(\frac{dp}{dL}\right) - \tau_i S_i - \rho_c A_c \frac{g}{g_c}\sin\theta = 0 \qquad \text{Eq. 19}$$

The shear stresses for this case are given by:

$$\tau_{wL} = \frac{f_f\rho_L V_f^2}{2g_c}, \text{ and } \tau_i = \frac{f_i\rho_c\left(V_c - V_f\right)^2}{2g_c} \qquad \text{Eq. 20}$$

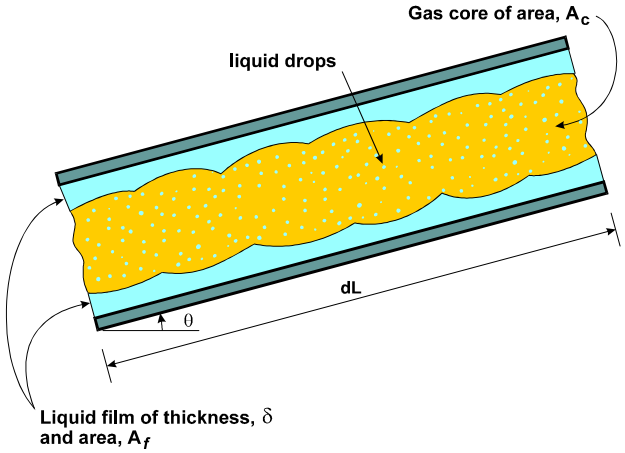

FIGURE 2 - CHARACTERISTICS OF ANNULAR-MIST FLOW

As was done for stratified flow, the following equation can be solved for the dimensionless film thickness, δ_L:

$$X^2F_2 - F_1 + 4Y = 0 \text{ where} \qquad \text{Eq. 21}$$

$$Y = \frac{(\rho_L-\rho_c)g\sin\theta}{\left(\frac{dp}{dL}\right)_{SG}g_c}$$

$$F_1 = \left(\frac{f_i}{f_{SG}}\right)\frac{\rho_c}{\rho_G}\tilde{V}_{cf}^2\tilde{S}_i\left(\frac{1}{\tilde{A}_f}+\frac{1}{\tilde{A}_c}\right)$$

$$F_2 = \left(\frac{f_f}{f_{SL}}\right)\tilde{V}_f^2\frac{\tilde{S}_L}{\tilde{A}_f} \text{ and } \tilde{V}_{cf} = \left(\frac{V_c - V_f}{V_{SG}}\right)$$

The velocities of the liquid film and of the gas core are given by:

$$V_f = V_{SL}(1-FE)\frac{A}{A_f} = V_{SL}\frac{(1-FE)}{4\tilde{\delta}\left(1-\tilde{\delta}\right)} \qquad \text{Eq. 22}$$

$$V_c = \left(V_{SG}+V_{SL}FE\right)\frac{A}{A_c} = \frac{\left(V_{SG}+V_{SL}FE\right)}{\left(1-2\tilde{\delta}\right)^2} \qquad \text{Eq. 23}$$

The friction factor for the liquid film, f_f, is evaluated from the single phase relationships at the film Reynolds number. The only additional quantities required are the interfacial friction factor, f_i, and the liquid fraction entrained, FE. To obtain appropriate correlations for these quantities, all the available annular-mist flow data were extracted from the Stanford Multiphase Flow Database (a total of 1,007 measurements) and the following procedure adopted.

By assuming that each experimental data point represented the desired pressure gradient and liquid volume fraction, a two-dimensional Newton-Raphson approximation was used to determine the values of f_i and FE that, when used with the model described herein, would produce these values. Some of the data were not able to converge to within the desired accuracy of 15% and were discarded.

The remaining 742 observations were used to obtain the following correlations for FE and f_i:

$$\frac{FE}{1-FE} = 3.523\left(\frac{V_{SL}}{V_{SG}+V_{SL}}\right)^{0.15} N_D^{0.11} N_L^{0.03} N_B^{0.074} \qquad \text{Eq. 24}$$

$$\frac{f_i}{f_c} = 5.91\left(\frac{\sigma}{\rho_c V_c^2 D_c}\right)^{0.25}\left(\frac{V_c}{V_c - V_f}\right)^{2.79} \mathrm{Re}_f^{0.103} \qquad \text{Eq. 25}$$

The dimensionless quantities are defined as:

$$N_L = \mu_L\left[\frac{g_c}{\rho_L \sigma^3}\right]^{1/4},\ N_B = \frac{\mu_L^2 V_{SG}^2 \rho_G}{\sigma^2 \rho_L},\ N_D = D\sqrt{\frac{\rho_L g_c}{\sigma}} \qquad \text{Eq. 26}$$

Barnea presents a model for the transition from annular flow based on two conditions. The first of these is based on the observation that the minimum interfacial shear stress is associated with a change in the direction of the velocity profile in the film. When the velocity profile becomes negative, stable annular flow cannot be maintained and the transition to intermittent flow occurs. The minimum shear stress condition may be determined from Eq. 18 to Eq. 20 by setting $\partial \tau_i / \partial \delta_L = 0$ and results in the following limit on Y:

$$Y_{\lim} = \frac{f_f}{f_{SL}}(1-FE)^2 \frac{\left(2-\frac{3}{2}E_f\right)}{E_f^3\left(1-\frac{3}{2}E_f\right)} X^2 \qquad \text{Eq. 27}$$

Note that this differs from the expression presented by Barnea which is based on the assumptions of no entrainment (FE=0) and smooth pipe friction factors based on the Blasius correlation.

The second mechanism proposed by Barnea for annular flow instability occurs when the supply of liquid in the film is sufficient to cause blockage of the gas core by bridging the pipe. This is said to take place when the in situ volume fraction of liquid exceeds one half of the value associated with the maximum volumetric packing density of gas bubbles (0.52). Hence, annular flow cannot exist when:

$$E_L \geq \tfrac{1}{2}(1-0.52) \text{ or } E_L \geq 0.24 \qquad \text{Eq. 28}$$

The liquid volume fraction is calculated from:

$$E_L = 1-(1-2\tilde{\delta}_L)^2 \frac{V_{SG}}{V_{SG}+FE\,V_{SL}} \qquad \text{Eq. 29}$$

The pressure drop may be obtained directly from the momentum balance equations once the liquid film thickness is known.

Intermittent Flow

The intermittent flow model used here includes the slug and elongated bubble flow patterns. It is characterized by alternating slugs of liquid trailed by long bubbles of gas. The liquid slug may contain dispersed bubbles and the gas bubbles have a liquid film below them. It is assumed that the flow is incompressible and that the film thickness is uniform. A schematic representation of this model is shown in Figure 3.

Assuming that the flow is incompressible and a uniform depth for the liquid film, the liquid volume fraction may be determined by writing an overall liquid mass balance over a slug-bubble unit[10]:

$$E_L = \frac{E_{Ls}V_t + V_{Gdb}(1-E_{Ls}) - V_{SG}}{V_t} \qquad \text{Eq. 30}$$

where V_{Gdb} represents the velocity of the dispersed bubbles, V_t is the translational velocity of the slug, and E_{Ls} is the volume fraction liquid in the slug body. All of these quantities need to be determined based on empirical correlations.

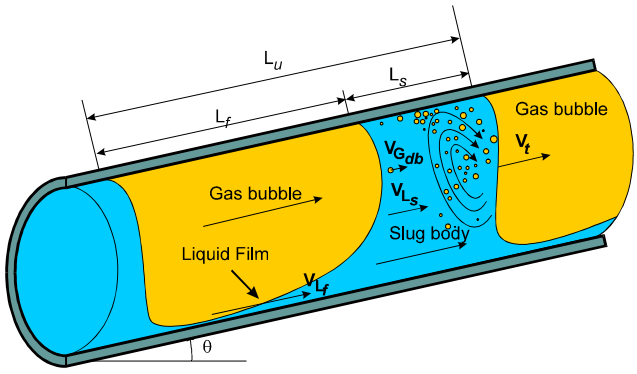

FIGURE 3 - INTERMITTENT FLOW MODEL

The liquid fraction in the slug E_{Ls} is calculated based on the Gregory[11] et al. correlation:

$$E_{Ls} = \frac{1}{1+\left(\frac{V_m}{8.66}\right)^{1.39}} \qquad \text{Eq. 31}$$

The translational velocity of the elongated bubbles is given by Bendiksen[8] as:

$$V_t = C_0 V_m + V_b \qquad \text{Eq. 32}$$

where the coefficient, C_0 is based on the Hughmark[12] correlation. It is approximately equal to 1.2 and approaches 2.0 as the flow becomes laminar. The bubble drift velocity, V_b, can be calculated from the Zuboski[19] correlation:

$$V_b = f_m V_{b_\infty} \qquad \text{Eq. 33}$$

$$\text{where } f_m = 0.316\sqrt{\mathrm{Re}_\infty} \text{ for } f_m < 1, \text{ otherwise } f_m = 1$$

$$\mathrm{Re}_\infty = \frac{\rho_L V_{b_\infty} D}{2\mu_L}$$

Bendiksen[8] gives the bubble drift velocity at high Reynolds numbers as:

$$V_{b_\infty} = V_{bh_\infty}\cos\theta + V_{bv_\infty}\sin\theta \qquad \text{Eq. 34}$$

The drift velocity of elongated bubbles in a horizontal system at high Reynolds numbers is given by Weber[17] as:

$$V_{bh_\infty} = \left[0.54 - \frac{1.76}{\mathrm{Bo}^{0.56}}\right]\sqrt{\frac{gD(\rho_L-\rho_G)}{\rho_L}}, \qquad \text{Eq. 35}$$

$$\text{where the Bond number, } \mathrm{Bo} = \frac{(\rho_L-\rho_G)}{\sigma} gD^2$$

Similarly, the drift velocity of elongated bubbles in a vertical system at high Reynolds numbers is given by Wallis[16] as:

$$V_{bv_\infty} = 0.345\left(1-e^{(0.337-0.1\,\mathrm{Bo})}\right)\sqrt{\frac{gD(\rho_L-\rho_G)}{\rho_L}} \qquad \text{Eq. 36}$$

Finally, the velocity of the dispersed bubbles in the liquid slug is obtained from the correlation of Ansari[2]:

$$V_{Gdb} = C_0 V_m + V_b E_{Ls}^{0.1} \qquad \text{Eq. 37}$$

$$V_b = 1.53\left[\frac{g(\rho_L-\rho_G)\sigma}{\rho_L^2}\right]^{\frac{1}{4}}\sin\theta$$

The pressure drop may be obtained by writing the momentum balance over a slug-bubble unit:

$$-\left(\frac{dp}{dL}\right) = \rho_m \frac{g}{g_c}\sin\theta + \frac{1}{L_u}\left[L_s\left(\frac{\tau_{Ls}\pi D}{A}\right) + L_f\left(\frac{\tau_{Lf}S_{Lf} + \tau_{Gdb}S_{Gdb}}{A}\right)\right] \quad \text{Eq. 38}$$

where the mixture density, $\rho_m = E_L\rho_L + E_G\rho_G$

The frictional pressure gradient in the gas bubble is normally small compared to that in the liquid slug. Furthermore, no reliable method is available for estimating terms required in the above equation for calculating the frictional pressure gradient in the bubble region. Xiao et al. have modeled this part of intermittent flow by assuming it to be analogous to stratified flow. This treatment contradicts observations made in the laboratory. In view of these uncertainties, the following simple approach is selected:

$$-\left(\frac{dp}{dL}\right) = \rho_m \frac{g}{g_c}\sin\theta + \left[\eta(E_L - 1) + 1\right]\frac{2f_{Lm}\rho_L V_m^2}{g_c D} \quad \text{Eq. 39}$$

where $f_{Lm} = f(\mathrm{Re}_{Lm}, \varepsilon_k)$, $\mathrm{Re}_{Lm} = \dfrac{D\rho_L V_m}{\mu_L}$

The calibration factor, η, is normally taken as 1.0.

Barnea proposes that the transition from intermittent flow occurs when the liquid fraction in the slug exceeds the value associated with the maximum volumetric packing density of the dispersed bubbles (0.52). The same mechanism is adopted in this model with the exception that the liquid volume fraction in the slug is obtained from Eq. 31, as opposed to the correlation proposed by Barnea.

Although it is not treated as a separate flow pattern for the purposes of phase volume fractions and pressure drop determination, the elongated bubble flow regime is defined here as the portion of intermittent flow for which the liquid slug contains no dispersed bubbles of gas. This condition is represented in the model by the region where $E_{L_s} \geq 0.90$

This model is appropriate for slight downward inclinations, where $\theta \geq 15°$, and for horizontal and uphill flow. For larger downward inclinations however, i.e. where $\theta \leq -15°$, the intermittent flow pattern is less well understood and not often observed. There are therefore insufficient data to support a mechanistic approach. In the present model, the method adopted is to treat this region as a transition zone existing between dispersed bubble and annular-mist. If stable annular-mist flow cannot be attained and the liquid rate is not sufficient to achieve dispersed bubble flow, the flow pattern is described as "Froth II" and an interpolation is performed between the liquid rates at the dispersed bubble and the annular-mist transitions.

Dispersed Bubble Flow

A simple homogeneous model is used to calculate the in situ phase volume fractions and pressure drop for this flow pattern. Holdup is neglected and the pressure drop is evaluated based on Moody's chart using the gas-liquid mixture properties.

The dispersed bubble flow region is bounded by two criteria. The first is based on the previously mentioned transition to slug flow, i.e. E_{ls}>0.48. The other criterion involves the transition to froth flow when the maximum volumetric packing density of the gas bubbles is exceeded:

$$C_G = \frac{V_{SG}}{V_m} > 0.52 \quad \text{Eq. 40}$$

Bubble Flow

Bubble flow can exist if the flow is intermittent and both of the following conditions are satisfied:

a) The Taylor bubble velocity exceeds the bubble velocity. This is satisfied in large diameter pipes (Taitel[14] et al.) when:

$$D > 19\left[\frac{(\rho_L - \rho_G)\sigma}{\rho_L^2 g}\right]^{\frac{1}{2}} \quad \text{Eq. 41}$$

b) The angle of inclination is large enough to prevent migration of bubbles to the top wall of the pipe (Barnea[7] et al.):

$$\cos\theta \leq \frac{3}{4\sqrt{2}}V_b^2\left(\frac{C_l\gamma^2}{g d_b}\right) \quad \text{Eq. 42}$$

The lift coefficient, C_l ranges from 0.4 to 1.2, the bubble distortion (from spherical) coefficient γ ranges from 1.1 to 1.5 and a bubble size, d_b between 4 and 10mm is recommended. For this model, C_l is taken as 0.8, γ as 1.3 and a bubble diameter of 7 mm is used.

When both of these conditions are satisfied, bubble flow is observed even at low liquid rates where turbulent forces do not cause bubble breakup. The transition to bubble flow from intermittent flow as suggested by Taitel[14] et al. occurs when the gas void fraction (during slug flow) drops below the critical value of 0.25.

Unrealistic flow pattern transitions have been observed when the line represented by Eq. 42 falls within the slug flow region. For this reason, the present model checks for the existence of bubble flow only within the elongated bubble flow regime.

Froth Flow

Froth flow represents a transition zone between dispersed bubble flow and annular-mist flow and between slug flow and annular-mist. In this model the reguon is labelled "Froth I", to distinguish it from the transition region, Froth II, described above. The approach used in this model is to interpolate between the appropriate boundary regimes in order to determine the transition values of the in situ liquid volume fraction and pressure drop. This involves a number of iterative procedures in order to determine the superficial gas velocities at the dispersed bubble, annular-mist and slug transitions to froth. Once V_{SG} at each transition is known, the volume fraction and pressure drop values *at the transitions* are calculated and a linear interpolation between these values is made for each quantity.

RESULTS

The evaluation of the model's performance has been performed using the following approaches.

The behavior of the model was examined over a wide range of flow rates and fluid properties using three-dimensional surface plots. This was done over the complete range of upward and downward pipe inclinations and both, pressure gradient and volumetric liquid fraction were analyzed. The results indicate generally smooth transitions between flow regimes.

In addition, data were extracted from the Stanford Multiphase Flow Database for which pressure gradient, holdup and flow pattern observations were available. This resulted in a total of 5,951 measurements consisting of variations in fluid properties pipe diameters and upward as well as downward inclinations. The model

predictions for liquid volume fraction are plotted against the experimental measurements in Figure 4. Figure 5 shows a similar plot for the pressure gradient calculations. A summary of all these results is also given in Table 1.

It can be seen that the model was able to predict the in situ liquid volume fraction to within an accuracy of 25% in 3,972 of the 5,951 cases (67%). The pressure gradient was predicted to the same accuracy for 2,970 cases (50%). The flow pattern prediction capabilities of the model are presented in

Table 2. The number of experimentally observed flow patterns are shown for each flow regime and these can be compared with the number predicted by the model. The third column represents the number of instances where the predicted flow pattern matched the experimental observations and it can be seen that a total of 1,843 predictions matched the experiments. It should be noted however, that due to the difficulty in classifying flow patterns near the transition zone, a significant number of the 1,322 Froth I predictions might have been reported as either slug or annular-mist.

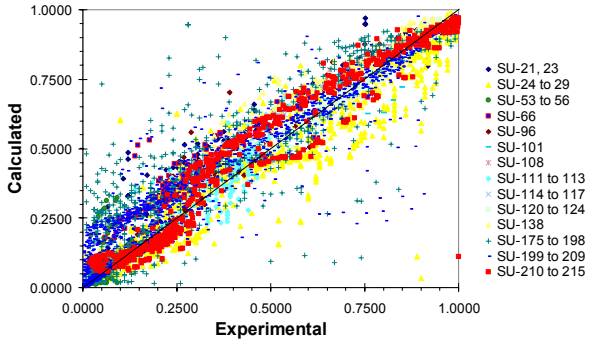

FIGURE 4 - COMPARISON OF CALCULATED LIQUID VOLUME FRACTION WITH EXPERIMENTAL DATA

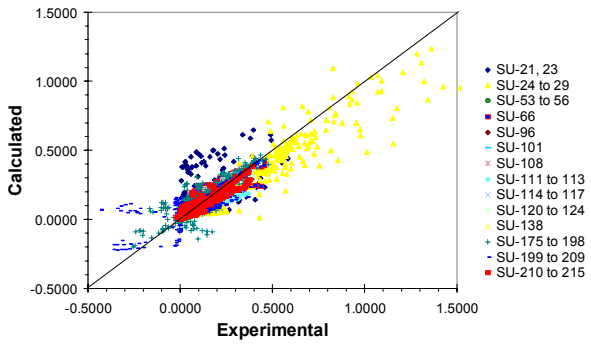

FIGURE 5 - COMPARISON OF CALCULATED PRESSURE GRADIENT WITH EXPERIMENTAL DATA

TABLE 1 - COMPARISON WITH EXPERIMENTAL DATA

			Cumulative			
	ΔP	E_L	ΔP		E_L	
Error	Count	Count	Count	%	Count	%
0-5%	1140	1633	1140	19%	1633	27%
5-10%	635	836	1775	30%	2469	41%
10-15%	469	643	2244	38%	3112	52%
15-20%	393	493	2637	44%	3605	61%
20-25%	333	367	2970	50%	3972	67%
25-30%	288	274	3258	55%	4246	71%
>30%	2693	1705				

TABLE 2 - FLOW PATTERN DISTRIBUTION IN EXPERIMENTAL DATA

Flow Pattern	Predicted	Measured	Matched
Elongated bubble	394	584	109
Bubble	43	426	0
Stratified smooth	148	449	99
Stratified wavy	670	563	163
Slug	1505	2103	627
Annular-Mist	1323	1007	656
Dispersed bubble	498	411	38
Froth I	1322	408	151
Froth II	48	0	0
Total	5951	5951	1843

SUMMARY AND CONCLUSIONS

A new mechanistic model has been presented which is applicable to all conditions commonly encountered in the petroleum industry. The model incorporates roughness effects as well as liquid entrainment, both of which are not accounted for by other models so far presented. The model has undergone extensive testing and has proven to be more robust that existing models and is applicable over a more extensive range of conditions.

While it is believed that significant improvements over existing models have been achieved, further research is needed to overcome problems associated with multiple roots and flow pattern transitions. Furthermore, empirical correlations necessary within the model can only be improved with accurate and consistent data over a wide range of conditions of commercial interest. Work in both of these areas is currently in progress.

ACKNOWLEDGEMENTS

The work described in this paper has been made possible through the support of the Reservoir Simulation Industrial Affiliates Program at Stanford University (SUPRI-B).

NOMENCLATURE

A	Cross-sectional area
D	Pipe internal diameter
E	In situ volume fraction
FE	Liquid fraction entrained
g	Acceleration due to gravity
h_L	Height of liquid (Stratified flow)
L	Length
p	Pressure

Re	Reynolds number
S	Contact perimeter
V_{SG}	Superficial gas velocity
V_{SL}	Superficial liquid velocity
δ_L	Liquid film thickness (Annular-Mist)
ε_k	Pipe roughness
θ	Angle of inclination
μ	Viscosity
ρ	Density
σ	Interfacial (surface) tension
τ	Shear stress
$\tilde{x}$	Dimensionless quantity, x

Subscripts

b	relating to the gas bubble
c	relating to the gas core
f	relating to the liquid film
db	relating to the dispersed bubbles
G	relating to the gas phase
i	relating to the interface
L	relating to the liquid phase
m	relating to the mixture
SG	based on superficial gas velocity
s	relating to the liquid slug
SL	based on superficial liquid velocity
wL	relating to the wall-liquid interface
wG	relating to the wall-gas interface

REFERENCES

1) Andritsos, N., "*Effect of Pipe Diameter and Liquid Viscosity on Horizontal Stratified Flow*," Ph.D. Dissertation, U. of Illinois at Champaign-Urbana (1986)
2) Ansari, A. M. "*A Comprehensive Mechanistic Model for Upward Two-Phase Flow*," M. S. Thesis, The University of Tulsa, 1987
3) Ansari, A. M., Sylvester, A. D., Sarica, C., Shoham, O., and Brill, J. P., "A Comprehensive Mechanistic Model for Upward Two-Phase Flow in Wellbores," SPE Prod. & Facilities, pp. 143-152, May 1994
4) Aziz, K. and Petalas, N., "New PC-Based Software for Multiphase Flow Calculations," paper SPE 28249 presented at the SPE Petroleum Computer Conference, Dallas, 31 July-3 August, 1994
5) Baker, A., Nielsen, K. and Gabb A., "New Correlations – 1, Pressure Loss Liquid-Holdup Calculations Developed," Oil & Gas J., March 14, 1988, 55-59
6) Barnea, D. "A Unified Model for Predicting Flow-Pattern transitions for the Whole Range of Pipe Inclinations," Int. J. Multiphase Flow, 13, No. 1, 1-12 (1987)
7) Barnea, D., Shoham, O.,Taitel, Y. and Dukler, A.E., "Gas-Liquid Flow in Inclined Tubes: Flow Pattern Transitions for Upward Flow," Chem. Eng. Sci., 40, 1 pp. 131-136 (1985)
8) Bendiksen, K. H. "An Experimental Investigation of the Motion of Long Bubbles in Inclined Pipes," Int. J. Multiphase Flow, 10, pp 1-12 (1984)
9) Colebrook, C. F., "Turbulent Flow in Pipes with Particular Reference to the Transition Region Between the Smooth and Rough-Pipe Laws," J. Inst. Civil Engrs., 11, 133 (1939)
10) Govier, G. W. and Aziz, K. "*The Flow of Complex Mixtures in Pipes*," Van Nostrand, Reinhold (1972), reprinted by Robert E. Kriger Publishing Co., Huntington, New York, 1977.
11) Gregory, G. A., Nicholson, M.K. and Aziz, K., "Correlation of the Liquid Volume Fraction in the Slug for Horizontal Gas-Liquid Slug Flow," Int. J. Multiphase Flow, 4, 1, pp. 33-39 (1978)
12) Hughmark, G. A., "Holdup and Heat Transfer in Horizontal Slug Gas Liquid Flow," Chem. Eng. Sci., 20, 1007-1010 (1965).
13) Oliemans, R. V. A., Pots, B. F., and Trope, N., "Modeling of Annular Dispersed Two-Phase Flow in Vertical Pipes," Int. J. Multiphase Flow, 12, No. 5, 711-732 (1986)
14) Taitel, Y., Barnea, D. and Dukler, A. E. "Modeling Flow Pattern Transitions for Steady Upward Gas-Liquid Flow in Vertical Tubes," AlChe Journal, 26, pp. 345-354 (1980)
15) Taitel, Y., and Dukler, A. E. "A Model for predicting Flow Regime Transitions in Horizontal and Near Horizontal Gas-Liquid Flow," AIChe Journal, 22, 47 (1976)
16) Wallis, G. B. "*One-Dimensional two-Phase Flow*," McGraw-Hill, New York, 1969
17) Weber, M. E., "Drift in Intermittent Two-Phase Flow in Horizontal Pipes," Canadian J. Chem. Engg., 59, pp. 398-399, June 1981
18) Xiao, J. J., Shoham, O., Brill, J. P., "A Comprehensive Mechanistic Model for Two-Phase Flow in Pipelines," paper SPE 20631, 65th ATC&E of SPE, New Orleans, September 23-26, 1990
19) Zukoski, E.E., "Influence of Viscosity, Surface Tension, and Inclination Angle on Motion of Long Bubbles in Closed Tubes," J. Fluid Mech., 25, pp. 821-837 (1966)